Hindawi
Adsorption Science & Technology
Volume 2023, Article ID 8122712, 12 pages
https://doi.org/10.1155/2023/8122712

Research Article

Adsorption of Cu(II) and Zn(II) onto Activated Carbon from Oil Palm Empty Fruit Bunch Prepared by Two-Step Acid Treatment and Microwave-Assisted Pyrolysis

Thotsaporn Somsiripan,[1] **Chayanoot Sangwichien**,[1] **Kanogwan Tohdee**,[2] **and Surat Semmad**[3]

[1]*Department of Chemical Engineering, Faculty of Engineering, Prince of Songkla University, Hat Yai, Songkhla 90112, Thailand*
[2]*Center of Excellence on Catalysis and Catalytic Reaction Engineering, Department of Chemical Engineering, Faculty of Engineering, Chulalongkorn University, Bangkok, Thailand*
[3]*Department of Construction Engineering, Faculty of Engineering and Architecture, Rajamangala University of Technology Tawan-ok, Bangkok, Thailand*

Correspondence should be addressed to Chayanoot Sangwichien; chayanoot.s@psu.ac.th

Received 16 January 2023; Revised 2 June 2023; Accepted 6 June 2023; Published 24 June 2023

Academic Editor: Szabolcs Pap

This study explores the feasibility of biochar-based activated carbon derived from oil palm empty fruit bunch (EFB) as a potential precursor for the preparation of activated carbon via 2-step H_3PO_4 activation under microwave-assisted pyrolysis (2ACEFB). The characterization of EFB and 2ACEFB was observed by FTIR and BET, and chemical composition was determined using proximate and elemental analysis data. The adsorptive removal of Cu(II) and Zn(II) from an aqueous solution was studied, and the effects of metal concentration and solution pH were also investigated. The pseudo-second-order equation was properly described, providing the best fit to the observed experimental data. The adsorption capacities of Cu(II) and Zn(II) onto the EFB were 20.28 and 18.06 mg/g, respectively, and improved by 2.04- and 1.89-fold onto the 2ACEFB. The potential of 2ACEFB was also proved by adsorbent reusability with five consecutive circles of the batch experiment without regeneration or treatment. This study demonstrated that 2ACEFB is an efficient adsorbent for eliminating heavy metals from aqueous solutions.

1. Introduction

The amount of heavy metals, harmful to humans and most animal species, is released from chemical industries such as the production of electric batteries, mining, and glass manufacturing factories. Several techniques, e.g., chemical reduction/precipitation, ion exchange, membrane separation, and adsorption, have been developed to eliminate heavy metal ions from wastewater. Among these techniques, adsorption is a widely used method for the removal of heavy metal ions due to more benefits that have been recognized, including high efficiency, easy handling, economic effectiveness, and the availability of many types of adsorbents [1–3].

In biomass adsorbents, activated carbons are excellent adsorbents because of their high performance with high surface area and a high degree of microporosity. However, the efficiency expected of the activated carbons dramatically depends on their precursors, activators, and treatment/production techniques. So, relatively expensive, nonrenewable precursors, including long-time heating production methods are a significant shortcoming for commercial activated carbon [2, 4]. Numerous researches have focused on different sources of adsorbent and found that the use of biological material is one of the most effective ways to use as precursors. The biological precursors (agricultural waste, biomass, etc.) have been considered an alternative and high-potential material for activated carbons due to their plenty and renewable nature [5]. Either with or without activation treatment, the initial process of activated carbon is required. Carbonization is the most widely used method, being a low-cost technique

in which organic matter can be transferred to elemental carbons by either conventional or microwave-assisted pyrolysis.

Microwave-assisted pyrolysis becomes advantageous because it provides a fast and selective heating mechanism [6] which can overcome many restrictions obtained from conventional heating regulation. Furthermore, during the microwave-assisted pyrolysis process, the media molecules hold a high frequency of vibration and frictional collision, resulting in a sudden increase in temperature. Thus, the treatment time can be decreased due to microwave energy. Numerous studies have shown that microwave-assisted pyrolysis can produce activated carbon with a higher specific surface area compared to conventional pyrolysis methods. This is due to the more rapid heating rates, which can lead to more efficient carbonization and activation of the material, resulting in a higher surface area and more uniform pore size distribution which can enhance its adsorption capacity "Microwave-assisted pyrolysis of coconut shell for production of activated carbon: Optimization using response surface methodology" [7], An et al. 2016 "Microwave-assisted pyrolysis of biomass for production of high-quality biooil and biochar with catalyst recycling by using activated carbon [8].

Biochar-based activated carbons have been used in several applications, providing high efficiency for sorption [9–11]. Acid activation is a simple and effective process, generally performed in one-step activation, for enhancing the adsorptive properties, functionalities, specific surface area, and selectivity of different adsorbates. Previously, two-stage activation was a process used in the preparation of activated carbon, providing more suitable activated carbon with a highly porous structure and useful functional groups for the removal of heavy metal ions from aqueous media (a novel route for the preparation of chemically activated carbon from pistachio wood for highly efficient Pb(II) sorption, activated carbon from wood wastes for the removal of uranium and thorium ions through modification with mineral acid). However, it is necessary to prove the efficiency of the produced activated carbon with different adsorbates. Therefore, this study attempted to examine the potential of activated carbons derived from palm oil empty fruit bunch via 2-step H_3PO_4 activation. The effects of different response parameters such as solution pH, metal ion concentration, and contact time were studied. The adsorption capacity of activated carbon as an adsorbent onto Cu(II) and Zn(II) was evaluated by a two- and three-parameter adsorption isotherm.

Heavy metals are toxic to the human body. Whether in the form of pure elements, organic compounds, and inorganic compounds, heavy metal's toxicity manifests itself when sufficient amounts are accumulated in the body. Copper and zinc are used mainly in the automotive and industrial paint industries. In the study of the removal of Cu(II) and Zn(II), the purpose was to use the synthesized activated carbon in the paint industry effluent treatment before releasing it into the natural water source.

2. Experimental and Methodology

2.1. Material and Chemicals. The oil palm empty fruit bunches utilized as raw materials in this investigation were collected in Surat Thani, South of Thailand. All of the substances used in this study were of analytical grade. Heavy metal salts $CuSO_4{\cdot}5H_2O$ and $Zn(NO_3)_2$, as well as H_3PO_4, purchased from Ajax Finechem and Loba Chemie, respectively, were utilized to prepare Cu(II) and Zn(II) stock solutions. Copper(II) sulfate pentahydrate ($CuSO_4{\cdot}5H_2O$) for analysis in EMSURE® and zinc standard solution traceable to SRM from NIST $Zn(NO_3)_2$ in HNO_3 0.5 mol/l 1000 mg/l Zn Certipur®.

Table 1: Physical and chemical composition of adsorbents.

Item	Sample	
	EFB	2ACEFB
BET surface area (m^2/g)	700.65	816.68
Pore volume (cm^3/g)	0.46	0.56
Pore size (Å)	32.16	22.43
Proximate analysis* (wt%)		
Moisture	4.82	6.15
Volatile	28.70	25.50
Fixed carbon	60.54	64.49
Ash	5.95	3.87
Ultimate analysis (wt%)		
C	71.44	79.25
N	2.23	2.10
O	26.33	14.11
P	—	4.54

*ASTM D7582-15 [17].

2.2. Adsorbent Preparation. Oil palm empty fruit bunches were gathered in Surat Thani, Southern Thailand, for usage as a raw material in this study. The activated carbon was made in the following processes: the raw materials were crushed and sieved into tiny sizes ranging from 1.0 to 2.0 mm and then pyrolyzed in a fixed bed reactor with flowing N_2 at 450°C for 1.5 hours, yielding biochar (hereafter named EFB) [12, 13]. The biochar was soaked in a phosphoric acid solution with a biochar/H_3PO_4 impregnation ratio of 1 : 1.75 (wt%) and periodic stirring [14]. The activation process was carried out at room temperature overnight. The resultant-activated carbon was obtained and then placed in the microwave-induced reactor for 10 min at 600 W and then washed with DI water until it reached pH 6-7. Overall activation processes were performed as duplicates, hereafter named 2ACEFB, in order to improve the adsorbent surface and adsorption efficiency, providing more efficacious [15].

2.3. Batch Adsorption. A series of batch experiments were conducted to evaluate the performance of 2ACEFB for the removal of Cu(II) and Zn(II) in an aqueous solution. Stock solutions were initially prepared by dissolving 3.929 g of $CuSO_4{\cdot}5H_2O$ and 2.896 g of $Zn(NO_3)_2$ in 1 L of distilled water. Standard metal solutions ranged 50-800 mg/L were then prepared appropriately by diluting the stock solution. Eventually, the pH of the metal solutions was adjusted by 0.1 M NaOH or HCl.

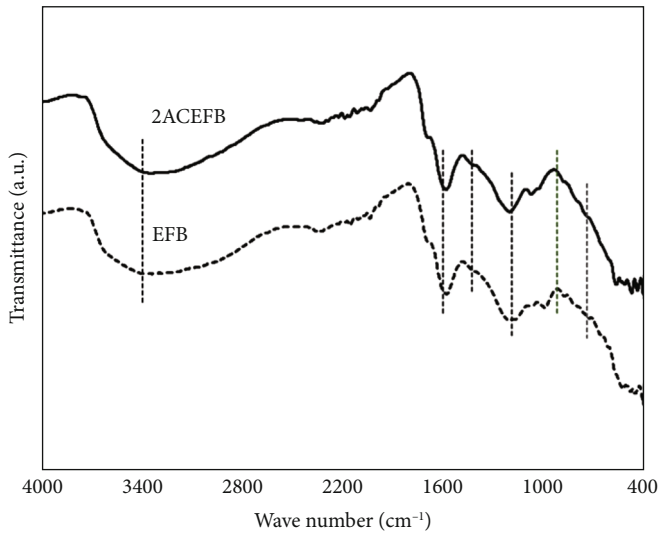

Figure 1: FTIR of untreated EFB and 2ACEFB.

In a batch adsorption study, 50 mL of prepared solution was placed in a 250 mL conical flask, and 1 g of adsorbent was added to the flask placing it in an incubator under 150 rpm at a controlled temperature (298 K). Factors affecting the adsorption efficiency such as pH solution (2-6), contact time (0, 10, 20, 40, 60, 90, 120, 180, 240, and 360 min), and initial metal concentration (12.5, 25, 50, 100, 150, 200, 300, 400, 600, and 800 mg/L) were intentionally investigated to determine the optimal condition, qualifying the adsorption and reusability performance of the adsorbent. The amount of adsorption adsorbed can be calculated as follow:

$$q_e = \frac{(C_o - C_e)V}{m}, \quad (1)$$

where q_e is the amount of metal ions adsorbed per mass of adsorbent at equilibrium (mg/g), V is the volume (L) of solution used for batch experiments, m is the mass (g) of adsorbent, and C_o and C_e are the initial concentration of metal ions and the equilibrium concentration of the solution (mg/g), respectively.

2.4. Instrumentation. The concentrations of Cu(II) and Zn(II) were measured by atomic absorption spectrophotometry (AAS) using AAnalyst 100 Spectrometer, PerkinElmer, Norwalk, CT/USA. EFB and 2ACEFB were characterized with an X-ray fluorescence spectrometer, PW2400, Philips, Netherlands. The FTIR spectra of the biochar EFB and 2ACEFB were recorded from KBr pellets with a Fourier transform infrared spectrometer, Vertex 70, Bruker, Germany. Surface area and porosity were determined using BET-technique, ASAP2460, Micromeritics, USA.

3. Result and Discussion

3.1. Chemical Composition and BET. The proximate analysis, in terms of moisture content, ash content, volatile matter, and fixed carbon, was carried out according to the ASTM standard. The result revealed that the composition of biochar EFB was 4.82 wt% moisture, 28.70 wt% volatile, 60.54 wt% fixed carbon, and 5.95 wt% ash (Table 1). It is clear that EFB contains high fixed carbon and low ash content, making it possible to be used as an activated carbon precursor [16]. After the 2-step H_3PO_4 treatment with a 1.75 impregnation ratio, the proximate composition of the 2ACEFB was 6.15 wt% moisture, 25.50 wt% volatile, 64.49 wt% fixed carbon, and 3.87 wt% ash.

The BET result showed that the surface area of 2ACEFB reached 816.68 m^2/g, an increase over biochar EFB, as shown in Table 1. This result is similar to those previously reported in the comprehensive literature [18, 19]. The pore volume of the adsorbent increased corresponding with a high surface area which can imply a large number of active sites, and the high mesopore volume enhances the mass transfer rate [19]. This behavior can be described as phosphoric acid acting as a template for creating microporosity during the activation stage [20].

3.2. Surface Functionality and Morphology. Carbon matric is a complex nature that not only consists of the carbon atom but is also formed by others such as oxygen, nitrogen, halogen, sulfur, and phosphorus. These heteroatoms are bonded to the carbon surface layer at the edges [18]. The FTIR spectra of biochar (EFB) and 2-step H_3PO_4-activated carbon (2ACEFB) are shown in Figure 1. The broadband at the peak of 3400 cm^{-1} corresponds to the –OH groups, hydroxyl groups from carboxyls, phenols, and adsorbed water [21, 22]. The band at 2922 cm^{-1} is due to the C–H stretching of methyl and methylene groups [21]. The region of the spectrum 1300 and 900 cm^{-1} consists of different bands being assigned to the C–O stretching in acids, alcohols, phenols, ethers, and esters found in oxidized carbons. However, it is noteworthy to mention that the phosphorous and phosphorous carbonaceous compounds existing in the phosphoric acid-activated carbon are presented in the band region between 900 and 1300 cm^{-1} [22].

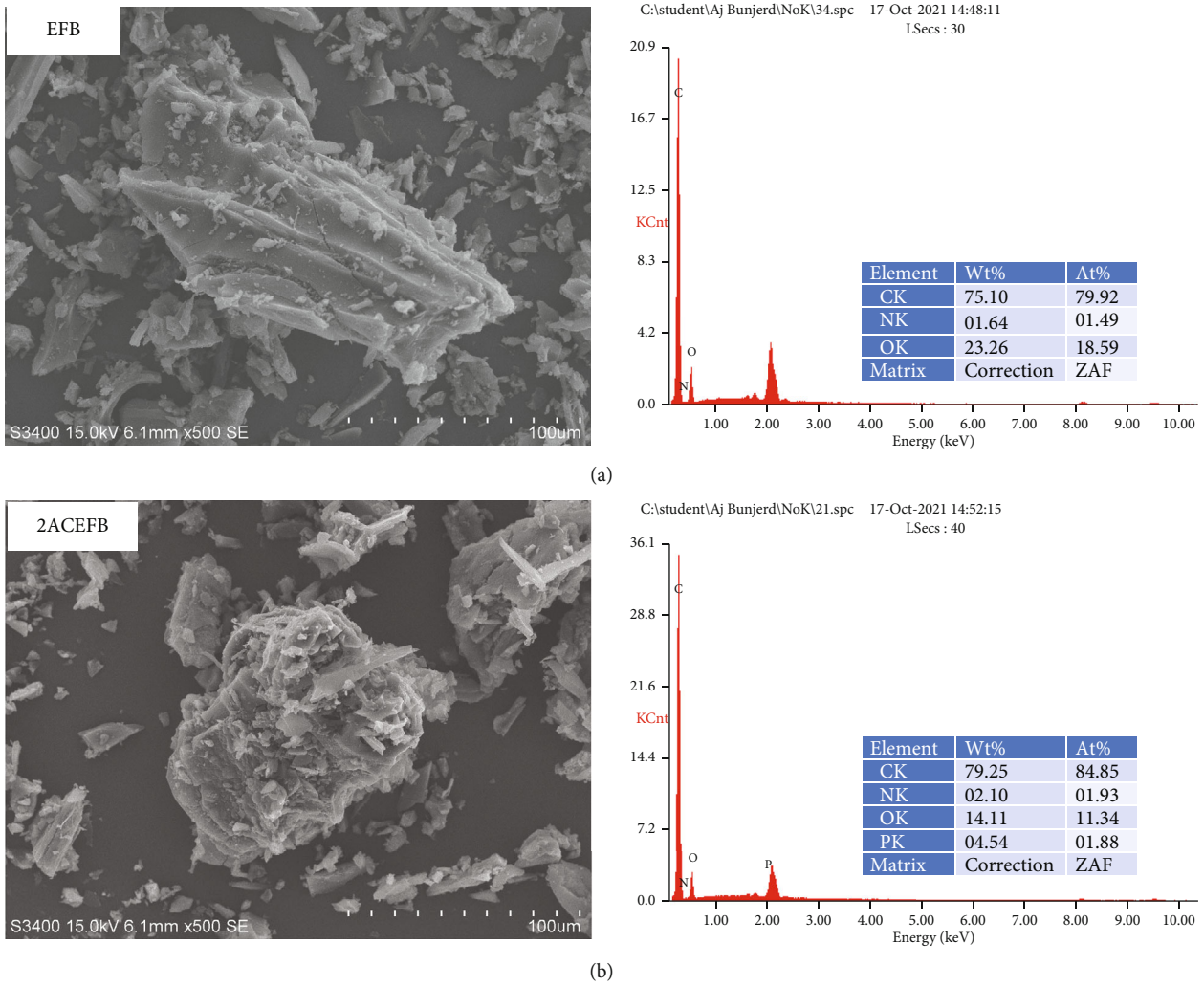

Figure 2: SEM-EDS of EFB and 2ACEFB.

Table 2: Nonlinear and linearized form of the kinetic models.

Kinetic model	Nonlinear form	Linearized form	Model parameters
Pseudo-first-order	$q_t = q_e - q_e e^{-k_1 t}$	$\log(q_e - q_t) = \log q_e - \frac{k_1 t}{2.303}$	q_e, k_1
Pseudo-second-order	$q_t = \frac{k_2 q_e^2 t}{1 + k_2 q_e t}$	$\frac{t}{q_t} = \frac{1}{k_2 q_e^2} + \frac{t}{q_e}$	q_e, k_2

Table 3: Kinetic model parameters of Cu(II) and Zn(II) onto EFB and 2ACEFB.

Kinetic model	Parameters	Adsorbent-adsorbate			
		EFB-Cu	2ACEFB-Cu	EFB-Zn	2ACEFB-Zn
Pseudo-first-order model	k_1 (min^{-1})	0.0584	0.0584	0.0417	0.0533
	q_e (mg/g)	8.63	8.57	8.13	8.45
	R^2	0.974	0.974	0.960	0.962
Pseudo-second-order model	k_2 (min^{-1})	0.0094	0.0138	0.0109	0.0102
	q_e (mg/g)	9.26	9.12	8.47	9.22
	R^2	0.998	0.999	0.998	0.998

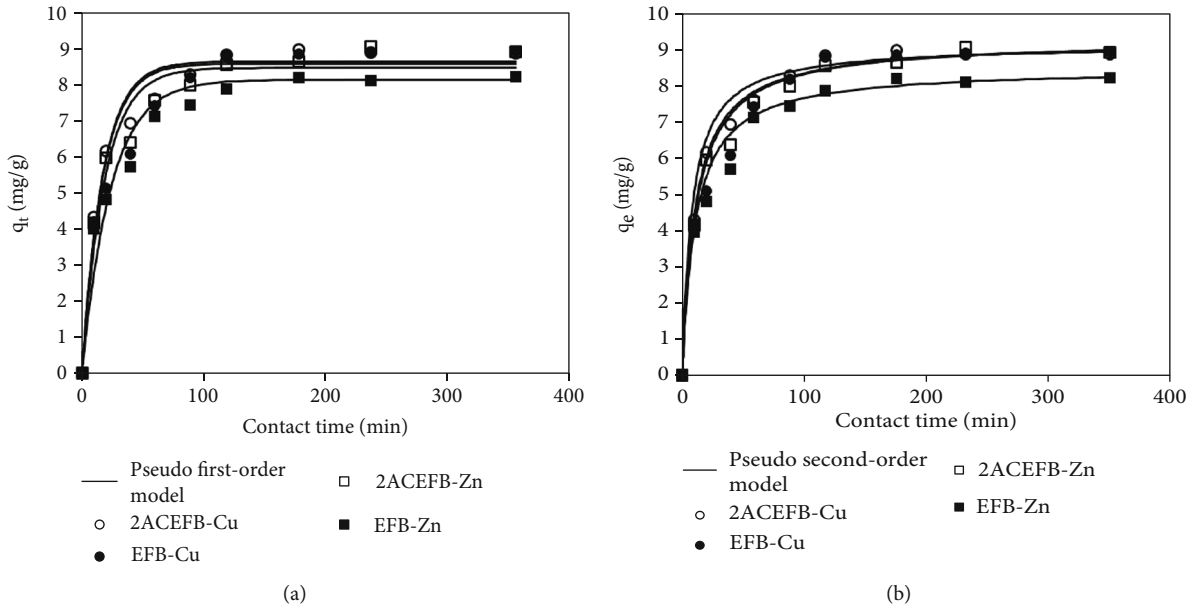

Figure 3: Nonlinear fitting of pseudo-first (a) and second-order models (b) of Cu(II) and Zn(II) onto EFB and 2ACEFB.

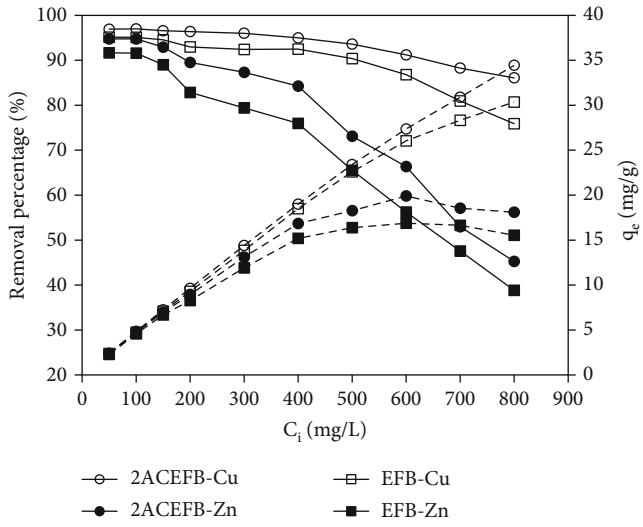

Figure 4: Effect of initial metal ion concentration (solid and dashed line represented removal percentage and metal uptake, respectively).

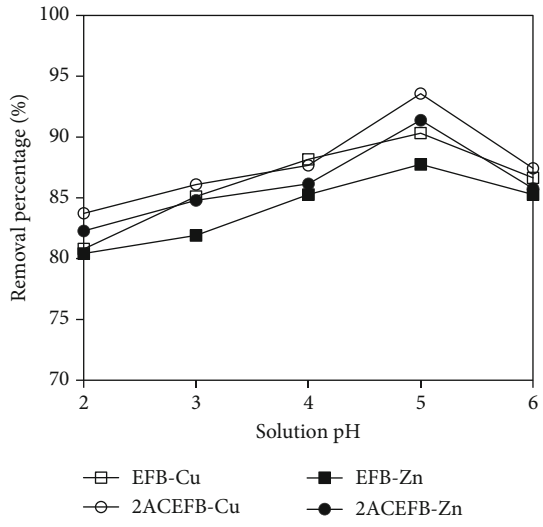

Figure 5: Effect of pH solution.

The morphology of empty fruit bunches (EFB) demonstrates a surface that is heterogeneous, containing varying amounts of debris which arise as a consequence of the pyrolysis process. The imaging utilizing energy-dispersive X-ray spectroscopy (EDS) indicated the existence of several organic components, including phosphorus, which has the potential to be incorporated in the formation of a phosphate skin on the surface of EFB after the treatment with phosphate acid (Figure 2).

3.3. Adsorption Kinetics. To examine the controlling mechanism of the adsorption process, the adsorption data were evaluated in terms of pseudo-first- and second-order-kinetic models. [23] The model expressions in terms of nonlinear and linearized forms are shown in Table 2.

The results revealed that models were relevant to the experimental data with a coefficient of determination (R^2) of data with a coefficient of determination (R^2) was more than 0.95. However, the kinetics of Cu(II) and Zn(II) onto EFB and 2ACEFB were adequately described by the pseudo-second-order model, in which the kinetic parameters determined are tabulated in Table 3. It can be seen from Figure 3, a nonlinear plot with the kinetic parameters from Table 3, that a relationship between the adsorption uptake (q_e) from the experiments ($q_{e,\exp}$) and the calculated value ($q_{e,\mathrm{cal}}$) was a good fit with R^2 ranged from 0.998 to 0.999. This means that the

Table 4: Expression of two-parameter and three-parameter isotherm models.

Isotherm model	Nonlinear form	Linearized form	Model parameters
Two-parameter model			
Langmuir	$q_e = \frac{q_m K_L C_e}{1 + K_L C_e}$	$\frac{1}{q_e} = \frac{1}{q_m} + \frac{1}{K_L q_m C_e}$	K_L, q_m
Freundlich	$q_e = K_F C_e^{1/n}$	$\ln_{q_e} = \ln_{K_F} + \frac{1}{n} \ln C_e$	K_F, n
Temkin	$q_e = \frac{RT}{b_T} \ln (K_T C_e)$	$q_e = \frac{RT}{b_T} \ln (K_T) + \frac{RT}{b_T} \ln (C_e)$	K_T, b_T
Three-parameter model			
Redlich-Peterson	$q_e = \frac{AC_e}{1 + BC_e^g}$	—	A, B, g
Sips model	$q_e = \frac{q_{mS} K_S C_e^{mS}}{1 + K_S C_e^{mS}}$	—	q_{mS}, K_S, mS
Toth model	$q_e = \frac{q_{mT} C_e}{\left((1/K_T) + C_e^{mT}\right)^{1/mT}}$	—	q_{mT}, K_T, mT

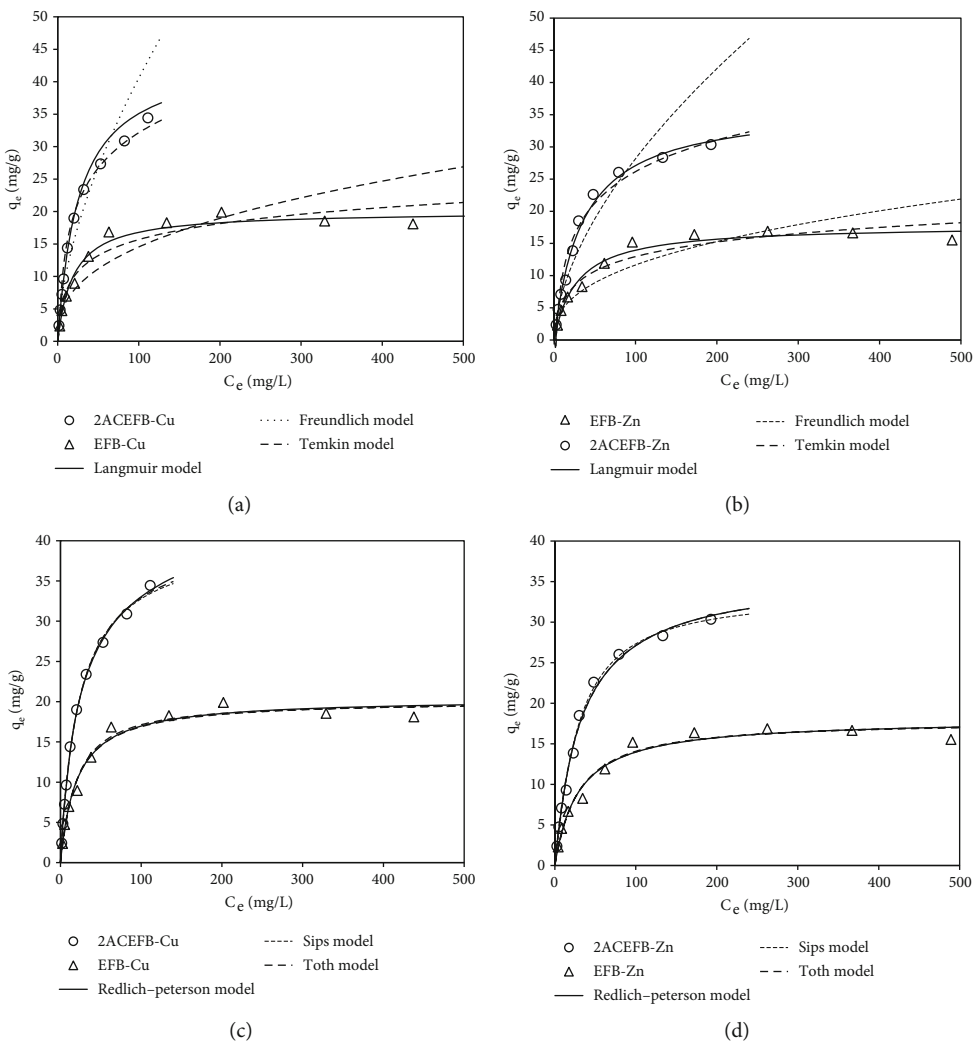

Figure 6: Nonlinear data fitting of isotherm models for Cu(II) and Zn(II) adsorption onto EFB and 2ACEFB under optimal condition for (a, b) a two-parameter model and for (c, d) three parameters.

Table 5: Isotherm parameters for the adsorption of Cu(II) and Zn(II) onto EFB and 2ACEFB.

Isotherm model	Parameters	Adsorbent-adsorbate			
		EFB-Cu	2ACEFB-Cu	EFB-Zn	2ACEFB-Zn
Two-parameter model					
Langmuir	K_L	0.052	0.038	0.036	0.029
	q_m	20.02	44.29	17.82	36.43
	R^2	0.997	0.996	0.997	0.997
	MAPE	6.11	3.80	6.28	4.60
Freundlich	K_F	2.51	2.58	1.920	1.93
	n	2.62	1.67	2.55	1.72
	R^2	0.929	0.955	0.885	0.929
	MAPE	20.58	15.35	18.38	16.56
Temkin	K_T	315.97	350.21	697.39	757.95
	b_T	0.604	0.403	0.825	0.527
	R^2	0.984	0.972	0.937	0.964
	MAPE	11.27	18.65	75.52	48.41
Three-parameter model					
Redlich-Peterson	A	1.009	1.938	0.621	1.101
	B	0.049	0.066	0.034	0.031
	g	1.000	0.9336	1.000	1.000
	R^2	0.977	0.998	0.971	0.993
	RMSE	2.985	1.327	2.824	2.651
	MAPE	6.05	3.41	6.41	4.82
Sips model	q_{mS}	20.01	41.66	17.80	33.58
	K_S	0.040	0.046	0.030	0.022
	mS	1.088	0.955	1.053	1.150
	R^2	0.978	0.998	0.972	0.995
	RMSE	2.918	1.484	2.805	2.294
	MAPE	7.97	3.21	7.57	7.26
Toth model	q_{mT}	20.28	40.67	18.06	36.00
	K_T	0.053	0.045	0.034	0.031
	mT	0.987	0.987	1.000	1.000
	R^2	0.976	0.997	0.971	0.993
	$RMSE$	3.016	1.555	2.82	2.66
	$MAPE$	6.02	2.41	6.41	4.82

pseudo-second-order model can be appropriately used to describe the adsorption kinetics. The amount of uptake for all experiments reached 84% by 60 min and gradually increased to the equilibrium time of 240 min. However, to ensure equilibrium uptake, 360 min equilibration time was used when determining the adsorption isotherms in the next section.

3.4. Effect of Concentration. Figure 4 illustrates the relationship of metal ion concentrations for Cu(II) and Zn(II) removals at equilibrium. The overall response shapes are similar across all cases, but 2ACEFB was a better adsorbent than EFB at high concentrations of heavy metals. The maximal improvement in removal by adsorption on comparing 2ACEFB to EFB was 40.80 and 37.04% for Cu(II) and Zn(II), respectively. This is due to the fact that high metal concentration provides a higher driving force for the transfer process to overcome the mass transfer resistance [24–26].

3.5. Effect of Solution pH. Solution pH is an essential factor that can affect the adsorption process. In fact, chemical precipitation became a dominant process for metal removal at pH 7 [27]. This condition was not solely considered as adsorption because the metal precipitation may lead to a misinterpretation of adsorption capacity. The effect of pH on metal Cu(II) and Zn(II) adsorption onto EFB and 2ACEFB was shown in Figure 5. The result revealed that the maximal adsorption of Cu(II) and Zn(II) onto the adsorbents was at pH 5.0. This result had a similar trend with adsorption study on several metal ions reported by numerous studies [26, 28, 29]. Therefore, the optimal condition used to determine the adsorption capacity of EFB and 2ACEFB was as follows: 1 g of adsorbent dose, pH 5, contact time of 360 min, and room temperature.

3.6. Adsorption Isotherm. Adsorption data were evaluated by both two-parameter (Langmuir, Freundlich, and Temkin) and three-parameter (Redlich-Peterson, Sips model, and

Table 6: Adsorption capacity of activated carbon with various raw materials toward heavy metals.

Heavy metal	Raw material	Adsorbent dose (g/L)	pH	Q_m (mg/g)	Best fit isotherms model	Reference
Cu(II)	Tahiti lemon peels	—	—	28.85	Langmuir	[36]
	Green vegetable waste	0.6	3.5	75.0	Langmuir	[37]
	Water hyacinth	12	6	3.53	Langmuir	[38]
	Pomelo peels	0.25	5	151.35	Langmuir	[39]
	Sugarcane bagasse	2	4.5	225	Langmuir	[40]
	Sewage sludge	0.5	5	26.06	Langmuir-Freundlich	[41]
	Banana leaves	2	5	66.2	Langmuir	[42]
	Calcium-rich biochars	1	5	141.76	Langmuir	[43]
	Raw cow manure	1.25	5	41.83	Freundlich	[44]
	Henna leaves	1.2	7	3.65	Langmuir	[45]
	Agricultural waste	3	9	56.2	Freundlich	[46]
	Oil palm empty fruit bunch	1	5	44.29	Langmuir	This study
Zn(II)	Coconut shell based	1	12	7.87	Langmuir	[47]
	Macadamia nutshell	0.3	4	22.73	Langmuir	[48]
	Water hyacinth	12	6	9.42	Langmuir	[38]
	Chlorella sp.	0.5	6	24.76	Langmuir	[49]
	Palm kernel shell	15.5	5	44.8	Langmuir	[50]
	Oil palm empty fruit bunch	1	5	36.43	Langmuir	This study

Toth model) isotherm models. Each model explains a specific feature of the adsorption process, and the model expressions and linearized forms are presented in Table 4. To examine the adsorption data, the mean absolute percentage error (MAPE) was used to quantify the experimental results compared with these isotherm models, which can be expressed as follows:

$$\mathrm{MAPE}(\%) = \frac{\sum_{i=1}^{N} \left| \left(q_{e,\exp} - q_{e,\mathrm{pre}} \right) / q_{e,\exp} \right|}{N} \times 100, \quad (2)$$

where $q_{e,\exp}$ and $q_{e,\mathrm{pre}}$ are the experimental and predicted uptake capacity (mg/g) and N is the number of data points.

The adsorption study results are illustrated in Figure 6, and associated parameters are tabulated in Table 5. Linear regression analysis was used to evaluate two-parameter isotherm models, providing the parameters used for nonlinear fitting. The experimental data fitted well with the Langmuir isotherm better than others, whose correlation coefficients were 0.996-0.997, suggesting that the mechanism was monolayer adsorption. The assumption of the Langmuir model involves an account of the formation of a monolayer of adsorbate molecules on the adsorbent surface. This is consistent with the assumption that the adsorption occurs at specific sites on the adsorbent surface [30].

The selected three-parameter models were fitted with the same experimental data (see Table 6). These three-parameter models provided good fits which MAPE ranged 2.41-7.97% was better than for the two-parameter isotherms (MAPE ranged 3.80-75.52%) for all experiments. It is also noteworthy that the parameters g, m_S, and m_T in the Redlich-Peterson, Sips, and Toth models, respectively, were approximately close to unity. This study result suggested that the adsorption of Cu(II) and Zn(II) onto 2ACEFB and EFB can be properly described by the Langmuir model with a homogenous surface.

3.7. Maximal Adsorption Capacity. For comparison propose of available model types, the three-parameter models obviously fit with the experimental data better than the two-parameter type in the range of initial concentration used and also supported the two-parameter Langmuir isotherm appropriately. It has been clearly shown that the adsorptive potential of Cu(II) was stronger than that of Zn(II). The maximal adsorption capacity of EFB onto Cu(II) and Zn(II) was observed as 20.01-20.28 and 17.80-18.06 mg/g, respectively. When EFB was activated by H_3PO_4, the adsorption capacity improved 2.04- and 1.886-fold to 40.67-41.66 and 33.58-36.00 mg/g over EFB (Table 5). The Cu(II) and Zn(II) uptake capacities obtained from this study are compared to relevant prior studies in the literature presented in Table 6. Therefore, it is concluded that the two-step acid treatment by H_3PO_4 improved both the physical and chemical properties, which can become more wealth capacity in Cu(II) and Zn(II) removal over untreated biochar from EFB.

3.8. Adsorption Mechanism. The surface functional groups of an adsorbent play a vital role in establishing a connection between the adsorbent and the adsorbate [31, 32]. Upon conducting FTIR analysis, it was observed that the process of phosphorylation resulted in an increase in porosity, carbon surface area, and the presence of carboxyl (-COOH) groups. Moreover, the introduction of the phosphoric acid group in 2ACEFB expanded the pore structure during the adsorption of Cu(II) and Zn(II), thus enhancing the

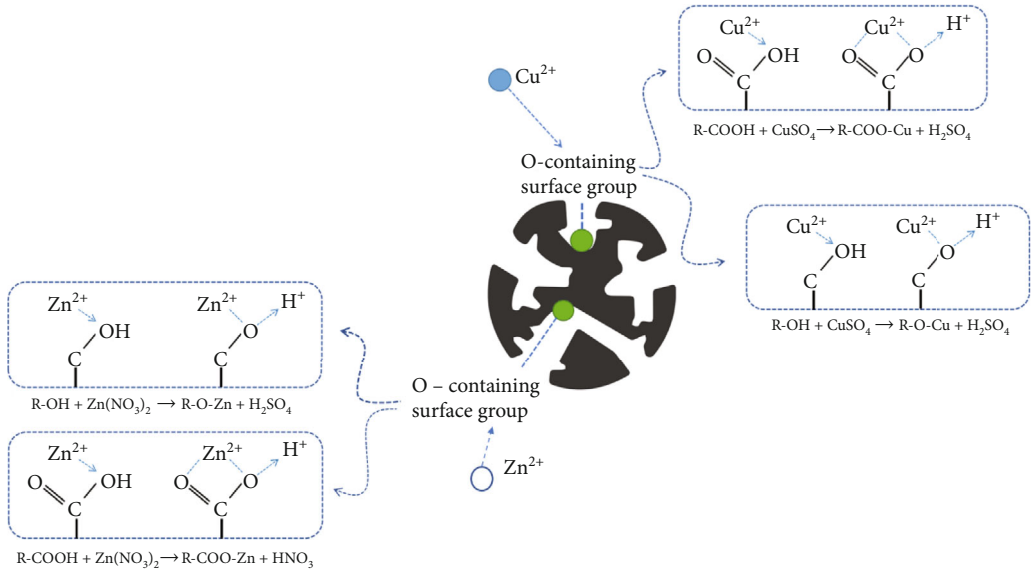

Figure 7: A proposed mechanism of the adsorption process of Cu(II) and Zn(II) onto activated carbon. $R\text{-}OH+CuSO_4 \longrightarrow R\text{-}O\text{-}Cu+H_2SO_4$. $R\text{-}COOH+CuSO_4 \longrightarrow R\text{-}COO\text{-}Cu+H_2SO_4$. $R\text{-}OH+Zn(NO_3)_2 \longrightarrow R\text{-}O\text{-}Zn+HNO_3$. $R\text{-}COOH+Zn(NO_3)_2 \longrightarrow R\text{-}COO\text{-}Zn+HNO_3$.

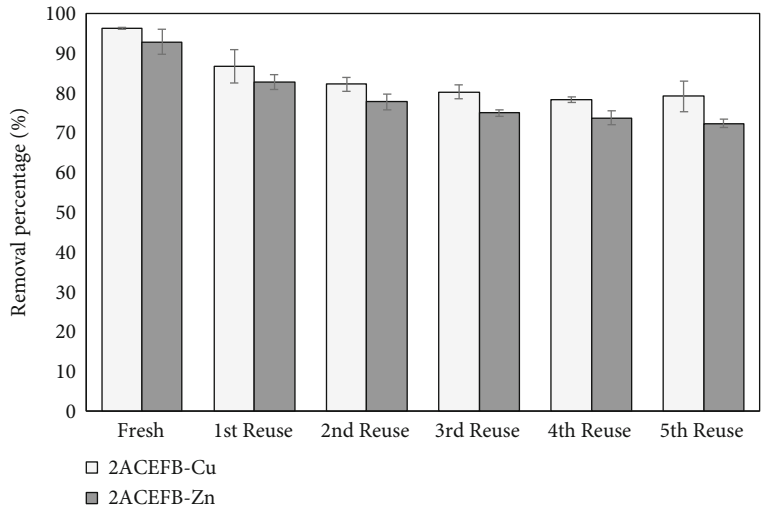

Figure 8: Effect of adsorbent reuse cycle on the removal of Cu(II) and Zn(II).

exposure of anions on the surface. This leads to an increased ability of 2ACEFB to adsorb Cu(II) and Zn(II) cations. According to Kriaa et al. [33], P-containing surface groups play a critical role in the adsorption of Cu(II) and Zn(II) in solution. This result is in agreement with earlier studies which demonstrated a strong correlation between the quantities of carboxylic phosphate groups, pyrophosphate groups, and the adsorption capacities of Cu(II) and Zn(II) [34, 35]. Figure 7 illustrated the scheme of Cu(II) and Zn(II) adsorption mechanism using phosphorylated sorbents in an aqueous solution, which can be summarized as follows.

3.9. Adsorbent Reusability. Adsorbent reusability is considered to be a significant advantage in determining the adsorbent's feasibility for practical application [51]. The reusability of the adsorbent in this study was accessed using a series of adsorption reactions under the similar conditions mentioned above (25°C temperature, 6 hrs, 1 g of adsorbent, pH 5, concentration 200 mg/L) by five consecutive reactions. After each reaction was completed, the spent adsorbents were collected from an aqueous solution by filtration and were dried at 105° C.

It is revealed that the removal of Cu(II) and Zn(II) by 2ACEFB was obviously decreased to 79.26 and 72.41%, as shown in Figure 8, respectively, after five consecutive reactions, which indicated inferior reusability of the prepared adsorbents. This result was repeatedly confirmed by the FTIR, as shown in Figure 9. The phosphate groups (band P-OH 919 cm^{-1} and amino phosphonic acid functional group 1191 cm^{-1}) have not been significantly changed in band shedding (1st-5th reuse). There was a slight decrease

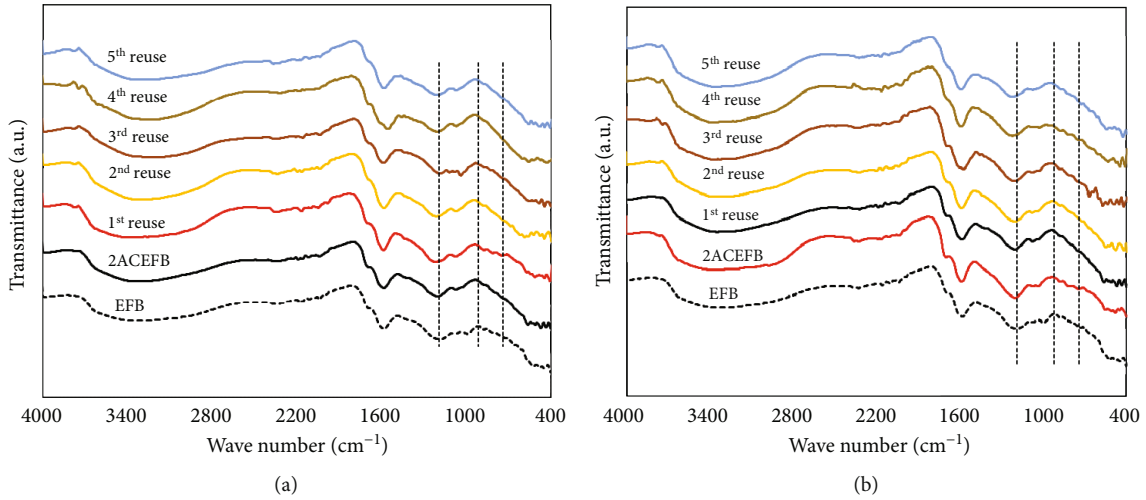

Figure 9: FTIR spectrum of 2ACEFB with five consecutive reactions. (a) Cu(II) and (b) Zn(II).

in the removal of Cu(II) and Zn(II) which may be due to the inferior reusability of the prepared adsorbent [52].

4. Conclusions

In this study, activated carbon was prepared via 2-step H_3PO_4 activation under microwave-assisted pyrolysis in order to examine its feasibility for the adsorption of Cu(II) and Zn(II) in an aqueous solution. A series of batch experiments was successfully done, and the conclusions can be drawn.

(1) The 2-step H_3PO_4-activated carbon (namely, 2ACEFB) derived by oil palm empty fruit bunch (EFB) was successfully performed in this study, totally proved by FTIR, BET, and proximate analysis. The specific surface area and pore volume of the adsorbent increase due to the H_3PO_4 activation

(2) Adsorption equilibrium reached 84% in approximately 60 min and developed to equilibrium time in 240 min for all cases. The pseudo-second-order model was the best description, with the coefficient of determination (R^2) ranged 0.998-0.999

(3) The 2ACEFB was clearly a better adsorbent than EFB, especially at high initial concentration, and improved the removal of Cu(II) and Zn(II) over EFB by 40.80 and 37.04% at pH 7, respectively. The maximal adsorption capacity of 2ACEFB was approximately 2.04- and 1.89-fold related to EFB, respectively, as described adequately by the Langmuir model with monolayer and homogenous surface adsorption

(4) The 2ACEFB showed good ability in adsorption reusability by five consecutive reactions, with the removal efficiency reduced to 79.26 and 72.41% for Cu(II) and Zn(II), respectively. Therefore, it is implied that the 2ACEFB acts as a promising adsorbent for metal ion adsorption

Data Availability

The data that support the findings of this study are available from the corresponding author, C.S., upon reasonable request.

Conflicts of Interest

The authors declare that they have no known competing financial interests or personal relationships that could have appeared to influence the work reported in this paper.

Authors' Contributions

Thotsaporn Somsiripan was responsible for the conceptualization, methodology, investigation, writing—original draft, and resources. Chayanoot Sangwichien was in charge of the conceptualization, and the validation, supervision, writing—review and editing, and funding acquisition. Kanogwan Tohdee contributed to the validation and formal analysis. Surat Semmad helped with the formal analysis.

Acknowledgments

The authors would like to acknowledge the financial support provided by the Prince of Songkla University Graduate School.

References

[1] B. H. Hameed, "Evaluation of papaya seeds as a novel non-conventional low-cost adsorbent for removal of methylene blue," *Journal of Hazardous Materials*, vol. 162, no. 2-3, pp. 939–944, 2009.

[2] V. K. Gupta, P. J. M. Carrott, M. M. L. Carrott, and R. Suhas, "Low-cost adsorbents: growing approach to wastewater

treatment—a review," *Critical Reviews in Environmental Science and Technology*, vol. 39, no. 10, pp. 783–842, 2009.

[3] N. Atar, A. Olgun, and S. Wang, "Adsorption of cadmium (II) and zinc (II) on boron enrichment process waste in aqueous solutions: batch and fixed-bed system studies," *Chemical Engineering Journal*, vol. 192, pp. 1–7, 2012.

[4] M. Jagtoyen and F. Derbyshire, "Some considerations of the origins of porosity in carbons from chemically activated wood," *Carbon*, vol. 31, no. 7, pp. 1185–1192, 1993.

[5] M. M. Rao, A. Ramesh, G. P. C. Rao, and K. Seshaiah, "Removal of copper and cadmium from the aqueous solutions by activated carbon derived from *Ceiba pentandra* hulls," *Journal of Hazardous Materials*, vol. 129, no. 1-3, pp. 123–129, 2006.

[6] W. A. Mahari, N. F. Zainuddin, W. M. N. Wan Nik, C. T. Chong, and S. S. Lam, "Pyrolysis recovery of waste shipping oil using microwave heating," *Energy*, vol. 9, no. 10, p. 780, 2016.

[7] K. Ismail, M. A. Ishak, Z. Ab Ghani et al., "Microwave-assisted pyrolysis of palm kernel shell: optimization using response surface methodology (RSM)," *Renewable Energy*, vol. 55, pp. 357–365, 2013.

[8] B. Zhang, Z. Zhong, Q. Xie, S. Liu, and R. Ruan, "Two-step fast microwave-assisted pyrolysis of biomass for bio-oil production using microwave absorbent and HZSM-5 catalyst," *Journal of Environmental Sciences*, vol. 45, pp. 240–247, 2016.

[9] M. Gale, T. Nguyen, M. Moreno, and K. L. Gilliard-AbdulAziz, "Physiochemical properties of biochar and activated carbon from biomass residue: influence of process conditions to adsorbent properties," *ACS Omega*, vol. 6, no. 15, pp. 10224–10233, 2021.

[10] J. Park, I. Hung, Z. Gan, O. J. Rojas, K. H. Lim, and S. Park, "Activated carbon from biochar: influence of its physicochemical properties on the sorption characteristics of phenanthrene," *Bioresource Technology*, vol. 149, pp. 383–389, 2013.

[11] P. D. Dissanayake, S. You, A. D. Igalavithana et al., "Biochar-based adsorbents for carbon dioxide capture: a critical review," *Renewable and Sustainable Energy Reviews*, vol. 119, article 109582, 2020.

[12] S. Choojit and C. Sangwichien, "Preparation of activated carbon production from oil palm empty fruit bunch and its application," *Kasem Bundit Engineering Journal*, vol. 8, no. 2, pp. 48–67, 2018.

[13] A. R. Mohamed, Z. Hamzah, and M. Z. Daud, "Optimization of the pyrolysis process of empty fruit bunch (EFB) in a fixed-bed reactor through a central composite design (CCD)," *AIP Conference Proceedings*, vol. 1605, no. 1, pp. 1172–1177, 2014.

[14] K. Y. Foo and B. H. Hameed, "Dynamic adsorption behavior of methylene blue onto oil palm shell granular activated carbon prepared by microwave heating," *Chemical Engineering Journal*, vol. 203, pp. 81–87, 2012.

[15] Y. Zhou, S. Niu, and J. Li, "Activity of the carbon-based heterogeneous acid catalyst derived from bamboo in esterification of oleic acid with ethanol," *Energy Conversion and Management*, vol. 114, pp. 188–196, 2016.

[16] D. Prahas, Y. Kartika, N. Indraswati, and S. Ismadji, "Activated carbon from jackfruit peel waste by H_3PO_4 chemical activation: pore structure and surface chemistry characterization," *Chemical Engineering Journal*, vol. 140, no. 1-3, pp. 32–42, 2008.

[17] ASTM Committee D-5 on Coal and Coke, *Standard Test methods for proximate analysis of coal and Coke by macro thermogravimetric analysis (ASTM D7582-15)*, ASTM International, 2010.

[18] S. M. Yakout and G. Sharaf El-Deen, "Characterization of activated carbon prepared by phosphoric acid activation of olive stones," *Arabian Journal of Chemistry*, vol. 9, pp. S1155–S1162, 2016.

[19] M. J. Valero-Romero, E. M. Calvo-Muñoz, R. Ruiz-Rosas, J. Rodríguez-Mirasol, and T. Cordero, "Phosphorus-containing mesoporous carbon acid catalyst for methanol dehydration to dimethyl ether," *Industrial & Engineering Chemistry Research*, vol. 58, no. 10, pp. 4042–4053, 2019.

[20] H. Marsh and F. Rodríguez-Reinoso, "Activation processes (chemical)," in *Activated Carbon*, vol. 6, pp. 322–365, Elsevier Science Ltd, Oxford, 2006.

[21] J. Yang and K. Qiu, "Preparation of activated carbons from walnut shells via vacuum chemical activation and their application for methylene blue removal," *Chemical Engineering Journal*, vol. 165, no. 1, pp. 209–217, 2010.

[22] A. M. Puziy, O. I. Poddubnaya, A. F. Martínez-Alonso, J. M. D. Suárez-García, and J. M. D. Tascón, "Surface chemistry of phosphorus-containing carbons of lignocellulosic origin," *Carbon*, vol. 43, no. 14, pp. 2857–2868, 2005.

[23] D. Pathania and S. Sharma, "Effect of surfactants and electrolyte on removal and recovery of basic dye by using Ficus carica cellulosic fibers as biosorbent," *Journal Tenside Surfactants Detergents*, vol. 49, no. 4, pp. 306–314, 2012.

[24] X. S. Wang, Y. P. Tang, and S. R. Tao, "Kinetics, equilibrium and thermodynamic study on removal of Cr (VI) from aqueous solutions using low-cost adsorbent alligator weed," *Chemical Engineering Journal*, vol. 148, no. 2-3, pp. 217–225, 2009.

[25] A. Mittal, V. K. Gupta, A. Malviya, and J. Mittal, "Process development for the batch and bulk removal and recovery of a hazardous, water-soluble azo dye (metanil yellow) by adsorption over waste materials (bottom ash and de-oiled soya)," *Journal of Hazardous Materials*, vol. 151, no. 2-3, pp. 821–832, 2008.

[26] K. Tohdee, *Enhancement of Cu(II), Zn(II), Ni(II) and humic acid adsorption in modified bentonite, [Ph.D. thesis]*, Prince of Songkhla University, 2018.

[27] T. Kanogwan and L. Kaewsichan, "Enhancement of adsorption efficiency of heavy metal Cu(II) and Zn(II) onto cationic surfactant modified bentonite," *Journal of Environmental Chemical Engineering*, vol. 6, no. 2, pp. 2821–2828, 2018.

[28] O. Abollino, A. Giacomino, M. Malandrino, and E. Mentasti, "Interaction of metal ions with montmorillonite and vermiculite," *Applied Clay Science*, vol. 38, no. 3-4, pp. 227–236, 2008.

[29] W. J. Chen, L. C. Hsiao, and K. K. Y. Chen, "Metal desorption from copper(II)/nickel(II)-spiked kaolin as a soil component using plant-derived saponin biosurfactant," *Process Biochemistry*, vol. 43, no. 5, pp. 488–498, 2008.

[30] H. Swenson and N. P. Stadie, "Langmuir's theory of adsorption: a centennial review," *Langmuir*, vol. 35, no. 16, pp. 5409–5426, 2019.

[31] J. C. Gómora-Hernández, M. D. Carreño-de-León, N. Flores-Alamo, M. D. Hernández-Berriel, and S. M. Fernández-Valverde, "Kinetic and thermodynamic study of corncob hydrolysis in phosphoric acid with a low yield of bacterial inhibitors," *Biomass and Bioenergy*, vol. 143, article 105830, 2020.

[32] Y. Huang, S. Li, J. Chen, X. Zhang, and Y. Chen, "Adsorption of Pb(II) on mesoporous activated carbons fabricated from water hyacinth using H_3PO_4 activation: adsorption capacity, kinetic and isotherm studies," *Applied Surface Science*, vol. 293, pp. 160–168, 2014.

[33] A. Kriaa, N. Hamdi, and E. Srasra, "Removal of Cu (II) from water pollutant with Tunisian activated lignin prepared by phosphoric acid activation," *Desalination*, vol. 250, no. 1, pp. 179–187, 2010.

[34] S. S. Choi, T. R. Choi, and H. J. Cho, "Surface modification of phosphoric acid–activated carbon in spent coffee grounds to enhance Cu(II) adsorption from aqueous solutions," *Applied Chemistry for Engineering*, vol. 32, no. 5, pp. 589–598, 2021.

[35] L. Wu, W. Wan, Z. Shang et al., "Surface modification of phosphoric acid activated carbon by using non-thermal plasma for enhancement of Cu(II) adsorption from aqueous solutions," *Separation and Purification Technology*, vol. 197, pp. 156–169, 2018.

[36] S. Pérez, M. Ulloa, E. Flórez et al., "Valorization of lemon peels wastes into a potential adsorbent for simultaneous removal of copper ion (Cu^{2+}) and Congo red from wastewater," *Environmental Nanotechnology, Monitoring & Management*, vol. 20, article 100795, 2023.

[37] M. I. Sabela, K. Kunene, S. Kanchi et al., "Removal of copper (II) from wastewater using green vegetable waste derived activated carbon: an approach to equilibrium and kinetic study," *Arabian Journal of Chemistry*, vol. 12, no. 8, pp. 4331–4339, 2019.

[38] B. C. Nyamunda, T. Chivhanga, U. Guyo, and F. Chigondo, "Removal of Zn (II) and Cu (II) ions from industrial wastewaters using magnetic biochar derived from water hyacinth," *Journal of Engineering*, vol. 2019, Article ID 5656983, 11 pages, 2019.

[39] Z. Liu and Y. Wei, "K_2CO_3-activated pomelo peels as a high-performance adsorbent for removal of Cu(II): preparation, characterization, and adsorption studies," *Journal of Chemistry*, vol. 2021, Article ID 9940577, 11 pages, 2021.

[40] T. E. Amoo, K. O. Amoo, O. A. Adeeyo, and C. O. Ogidi, "Kinetics and equilibrium studies of the adsorption of copper(II) ions from industrial wastewater using activated carbons derived from sugarcane bagasse," *International Journal of Chemical Engineering*, vol. 2022, Article ID 6928568, 24 pages, 2022.

[41] L. Fan, X. Wang, J. Miao et al., "$Na_4P_2O_7$-modified biochar derived from sewage sludge: effective Cu(II)-adsorption removal from aqueous solution," *Adsorption Science & Technology*, vol. 2023, Article ID 8217910, 15 pages, 2023.

[42] M. A. Darweesh, M. Y. Elgendy, M. I. Ayad, A. M. Ahmed, N. M. K. Elsayed, and W. A. Hammad, "Adsorption isotherm, kinetic, and optimization studies for copper (II) removal from aqueous solutions by banana leaves and derived activated carbon," *South African Journal of Chemical Engineering*, vol. 40, pp. 10–20, 2022.

[43] J. Liu, X. Yang, H. Liu, W. Cheng, and Y. Bao, "Modification of calcium-rich biochar by loading Si/Mn binary oxide after NaOH activation and its adsorption mechanisms for removal of Cu(II) from aqueous solution," *Colloids and Surfaces A: Physicochemical and Engineering Aspects*, vol. 601, article 124960, 2020.

[44] P. Zhang, X. Zhang, X. Yuan, R. Xie, and L. Han, "Characteristics, adsorption behaviors, Cu(II) adsorption mechanisms by cow manure biochar derived at various pyrolysis temperatures," *Bioresource Technology*, vol. 331, article 125013, 2021.

[45] T. Shanthi and V. M. Selvarajan, "Removal of Cr(VI) and Cu(II) ions from aqueous solution by carbon prepared from henna leaves," *Journal of Chemistry*, vol. 2013, Article ID 304970, 6 pages, 2013.

[46] G. Özsin, M. Kılıç, E. Apaydın-Varol, and A. E. Pütün, "Chemically activated carbon production from agricultural waste of chickpea and its application for heavy metal adsorption: equilibrium, kinetic, and thermodynamic studies," *Applied Water Science*, vol. 9, no. 3, p. 56, 2019.

[47] M. F. M. Yusop, E. M. J. Azmie, and M. A. Ahmad, "Single-stage microwave assisted coconut shell based activated carbon for removal of Zn(II) ions from aqueous solution - optimization and batch studies," *Arabian Journal of Chemistry*, vol. 15, no. 8, article 104011, 2022.

[48] M. T. Dao, T. P. L. Tran, D. T. Vo, V. K. Nguyen, and L. T. T. T. Hoang, "Utilization of macadamia nutshell residue for the synthesis of magnetic activated carbon toward zinc (II) ion removal," *Advances in Materials Science and Engineering*, vol. 2021, Article ID 2543197, 10 pages, 2021.

[49] M. Amin and P. Chetpattananondh, "Biochar from extracted marine *Chlorella* sp. residue for high efficiency adsorption with ultrasonication to remove Cr(VI), Zn(II) and Ni(II)," *Bioresource Technology*, vol. 289, article 121578, 2019.

[50] R. R. Karri and J. N. Sahu, "Modeling and optimization by particle swarm embedded neural network for adsorption of zinc (II) by palm kernel shell based activated carbon from aqueous environment," *Journal of Environmental Management*, vol. 206, pp. 178–191, 2018.

[51] E. H. Ezechi, S. R. . M. Kutty, A. Malakahmad, and M. H. Isa, "Characterization and optimization of effluent dye removal using a new low cost adsorbent: equilibrium, kinetics and thermodynamic study," *Process Safety and Environmental Protection*, vol. 98, pp. 16–32, 2015.

[52] P. Li, H. Jiang, A. Barr et al., "Reusable polyacrylonitrile-sulfur extractor of heavy metal ions from wastewater," *Advanced Functional Materials*, vol. 31, no. 51, article 2105845, 2021.